ChemComm

Accepted Manuscript

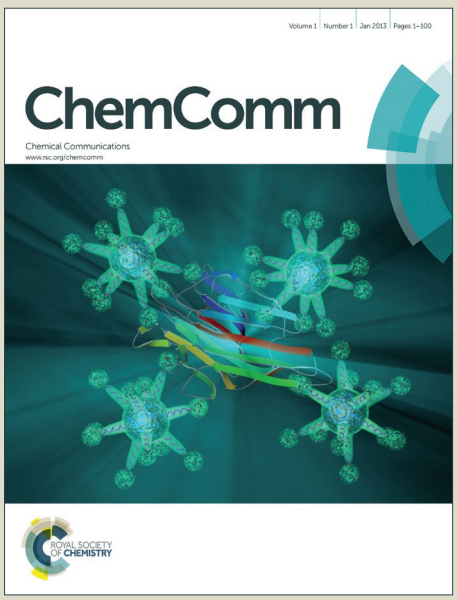

ROYAL SOCIETY OF CHEMISTRY

www.rsc.org/chemcomm

Journal Name

RSCPublishing

COMMUNICATION

Highly proton-conducting, methanol-blocking Nafion composite membrane enabled by surface-coating crosslinked sulfonated graphene oxide

Cite this: DOI: 10.1039/x0xx00000x

Received 00th January 2012,
Accepted 00th January 2012

DOI: 10.1039/x0xx00000x

www.rsc.org/

Guangwei He[ab], Xueyi He [ab], Xinglin Wang [a], Chaoyi Chang [a], Jing Zhao [ab], Zongyu Li[ab], Hong Wu[ab], and Zhongyi Jiang*[ab]

Coating an ultrathin crosslinked graphene oxide film onto Nafion support enables the successful overcoming of the tradeoff effect by the resulting composite membrane: 93% decrease of methanol permeability while retaining the high proton conductivity of Nafion, owing to the synergistic modulation of methanol-transport and proton-transport channels within the graphene oxide film.

Direct methanol fuel cell (DMFC) has received tremendous attention due to its high efficiency, environmental benignity and convenient fuel management.[1] For practical application, the proton exchange membranes (PEMs), one of the core components in DMFC, should possess both high proton conductivity and low methanol permeability. However, proton conductivity and methanol permeability are strongly coupled because of the high similarity and relativity in transport behavior between protons and methanol molecules in PEMs.[2] Protons transport along hydrogen bond network (primarily constructed by water), or diffuse with water in the form of hydronium ion. Methanol molecules self-diffuse as well as co-diffuse with water or protons. Thus, the transport of protons and methanol both depends on the morphology and chemical microenvironment of the water channels and water diffusion. Consequently, there exists a distinct tradeoff effect between proton conductivity and methanol permeability property, i.e., the membranes that exhibit high conductivity also exhibit high methanol permeability and vice versa. Apparently, due to the involvement of water except methanol and proton, this tradeoff effect becomes much more complicated.[3]

To disentangle this tradeoff effect, constructing an ultrathin graphene oxide (GO) film with tailored interlayer spacing and appropriate chemical microenvironment may be an ideal strategy. The past three years have witnessed encouraging breakthroughs of GO membranes in precisely separating a wide array of mixtures such as H_2/CH_4, CO_2/N_2, and H_2O/ethanol, indicating the potential of GO membrane as an emerging class of sieving membranes.[4-6] For example, Joshi et al. found that GO membrane in an ionic solution having a interlayer spacing of ~0.9 nm permits fast transport of ion or molecule with a hydrated radius of 0.45 nm or less, but rejects all larger sized species.[7] Such a precise sieving is rendered by the narrowly distributed channel size of GO membranes. Theoretically, ultralow methanol diffusion can be achieved through regulating the interlayer spacing of GO to prevent methanol from entering, while facilitated transport of much smaller protons can be achieved by constructing highly continuous ionic channels between GO nanosheets.[1] GO-based materials have been recently demonstrated as promising methanol-blocking coatings or fillers for PEMs.[8-11] Liu' group prepared Nafion/GO composite membranes by layer-by-layer deposition using 1, 4-phenyldiamine hydrochloride as crosslinker. The methanol permeability decreased by 96%, while the concomitant decline of proton conductivity by 82% was also observed.[8]

Herein, we prepared ultrathin GO film (~20 nm) crosslinked by 1, 4- phenylenediamine-2-sulfonic acid (PDASA) (Nafion/GO@PDASA) via spin-coating GO/PDASA (sodium salt form) solution on Nafion 212 support and subsequent thermal crosslinking and acidification. The resulting Nafion/GO@PDASA composite membrane successfully overcomes the tradeoff effect between proton conductivity and methanol permeability owing to the synergistic modulation of methanol-transport and proton-transport channels within the GO film. Specifically, the Nafion/GO@PDASA membrane exhibits a 93% decrease of methanol permeability while retaining the high proton conductivity of Nafion, rendering a dramatically high selectivity 12.9 times higher than that of Nafion.

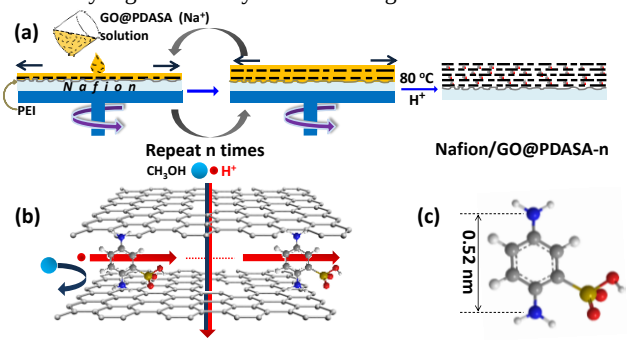

Fig. 1 (a) Fabrication of PDASA crosslinked GO film (GO@PDASA) by a spin-coating method; (b) Transport mechanism of proton and methanol through the GO@PDASA film; (c) Structure of 1, 4- phenylenediamine-2-sulfonic acid (PDASA).

Fig. 1 illustrates the fabrication of Nafion/GO@PDASA membrane. A spin-coating method[5, 12] is employed because of its

simplicity as well as its ability in affording GO film well-stacked, highly-interlocked microstructure with in-plane orientated GO nanosheets. PDASA is selected as the crosslinker considering the following three reasons: (i) the double primary amine groups can react with the epoxy groups on GO nanosheets during thermal treatment; (ii) the distance between the two nitrogen atoms of PDASA is 5.2 Å; such short distance may decrease the GO spacing, leading to high rejection of methanol molecules of GO film due to size exclusion effect; (iii) the sulfonic acid groups are superior proton-conducting groups, rendering the GO film high proton conductivity.

The successful synthesis of GO by the modified Hummers method was confirmed by atomic force microscope (AFM) and X-ray diffraction (XRD) characterization. The AFM image in Fig. S1a displays that the in-plane size of GO nanosheets is 0.5-1.5 μm, and the thickness of GO nanosheets is about 0.6 nm, which are in accordance with the GO synthesized in our previous studies.[13] The sharp peak (2θ=10.79) in XRD pattern (Fig. S1b) indicates that the interlayer spacing of GO nanosheets is 0.82 nm, which is very close to that of GO nanosheets reported in the literature.[13] The GO nanosheets show a lager interlayer spacing than that of graphite (about 0.33 nm) due to the presence of oxygen-containing functional groups and H_2O retained in the interlayer galleries of hydrophilic GO.[13]

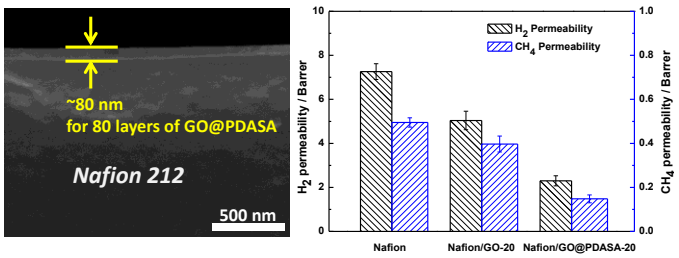

Fig. 2 (a) Thickness for 80 layers of GO@PDASA observed by SEM; (b) H_2 and CH_4 permeabilitie of Nafion, Nafion/GO-20 and Nafion/GO@PDASA-20 membranes.

The chemical structure of GO@PDASA film was identified by X-ray photoelectron spectroscopy (XPS). The XPS pattern **(**Fig. S1c**)** shows typical peaks of GO at binding energies of 282 and 530 eV, corresponding to C 1s and O 1s, respectively. The high content of oxygen (21.98 atom %) indicates a high oxidation degree of GO. The presence of peaks at 397 and 165 eV, which are assigned to N 1s and S 2p, respectively, validates the introduction of PDASA between GO nanosheets. According to the peak area of S 2p, the mass ratio of sulfur is calculated to be 1.5 wt%, corresponding to 0.47 mmol g^{-1} of sulfonated acid groups in GO@PDASA film. Compared with Fig. S4, it can be clearly observed that a thin film with a thickness about 80 nm appears on the top of Nafion support in Fig. 2a. This result indicates that the thickness of single layer of GO@PDASA is about 1 nm, in agreement with the thickness of single GO layer prepared by spin-coating method[12].

To verdict the variation of interlayer spacing of GO@PDASA, gas permeabilities through Nafion, Nafion/GO-20 and Nafion/GO@PDASA-20 membranes were measured, as shown in Fig. 2b. H_2 is selected as the probe molecule because its small kinetic diameter (0.289 nm) enables the accurate response of size variation of the interlayer channels; CH_4 is selected as the probe molecule because of its identical kinetic diameter (0.38 nm) with CH_3OH. After coating about 20 nm GO@PDASA film on Nafion 212 (51 μm) support, the H_2 and CH_4 permeabilities decrease by 68.3% (from 7.26 to 2.3 barrer) and 70.1% (from 0.495 to 0.148 barrer), respectively. The dramatic decrease of gas permeability caused by the ultrathin GO@PDASA film implies that the

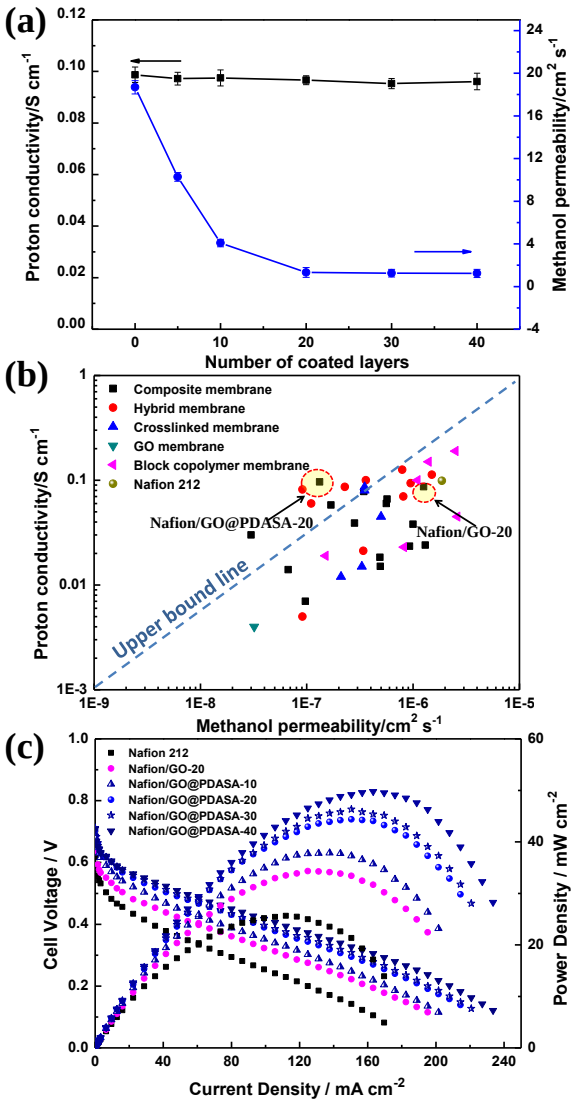

Fig. 3 (a) Proton conductivity (at 30 °C in water) and methanol permeability (at 30 °C) of Nafion/GO@PDASA membrane as a function of the number of spin-coated GO@PDASA layers; (b) Variations of proton conductivity *versus* methanol permeability for membranes in the literature and this study. The proton conductivity, methanol permeability and selectivity of these membranes are shown in Table S2 in the Supporting Information for better comparisons. (c) Polarization and power density curves of DMFCs. Operating conditions: Anode (2 M CH_3OH, 5 mL min^{-1}); Cathode (oxygen, 150 mL min^{-1}); Temperature (60 °C).

GO@PDASA film can block the gas transport by size exclusion mechanism.[5] Compared with Nafion/GO-20 membrane, Nafion/GO@PDASA membrane exhibits more remarkable decrease of the gas permeabilities, which are attributed to the reduction of interlayer spacing of GO after being crosslinked by PDASA and concomitant more pronounced size cutoff effect. Considering the identical kinetic diameter of CH_4 with CH_3OH, it can be anticipated that the reduction of interlayer spacing could afford excellent methanol-blocking property.

The methanol permeability (Fig. 3a) remarkably decreases by 93% with increasing the GO@PDASA layers from 0 to 20 layers, and further increase of GO@PDASA layers only slightly influence the

methanol-barrier property. The Nafion/@PDASA-20 membrane displays a methanol permeability of 1.32×10^{-7} cm^2 s^{-1}, 8.5 times lower than that of Nafion/GO-20 membrane (1.26×10^{-6} cm^2 s^{-1}, see Fig. 3b). Such obvious decrement of methanol permeability is in good accordance with the gas permeabilities for Nafion/@PDASA-20 and Nafion/GO-20 membranes, further verifying the reduction of interlayer spacing through crosslinking. In comparison with methanol permeability, the proton conductivity (Fig. 3a) of Nafion/GO@PDASA membranes is nearly identical to that of Nafion 212 membrane.

Fig. 3b summarizes the variations of proton conductivity *versus* methanol permeability for a variety of membranes. A tradeoff effect can be observed that membranes having high proton conductivity are often more permeable to methanol, and *vice versa*. Most of the membranes exhibit performance below the upper bound line, which is drawn empirically based on the experimental data in the corresponding figure. The Nafion/GO@PDASA-20 membrane successfully strides over the upper bound line due to the synergistic optimization of methanol-transport and proton-transport channels within the GO film (see the illustration in Fig. 1b). The main pathway for transporting both CH_3OH and protons are the interlayer channels within the GO film. Owing to the decreased interlayer spacing of GO@PDASA membrane, the Nafion/GO@PDASA membrane can effectively block the CH_3OH diffusion via size exclusion, as supported by the gas permeation experiment. It should be mentioned that CH_3OH could diffuse in the form of $(CH_3OH)_a$ and $(CH_3OH)_m(H_2O)_n$ clusters, which are more difficult to diffuse through the narrow channels within GO@PDASA film. The rational implementation of the size exclusion mechanism could hold the key to the much better methanol-blocking property of Nafion/GO@PDASA membrane than that of the documented membranes[14, 15], which reduce methanol permeability mainly via manipulating solution-diffusion mechanism. For the proton transport, the highly continuous channels between GO nanosheets, coupled with the appropriate chemical microenvironment (relatively high concentration of sulfonated acid groups (0.47 mmol g^{-1}) and abundant hydrophilic oxygen-containing groups (-COOH, -OH and epoxy groups)), could render well-connected water channels and rapid proton transport[1]; Moreover, unlike many other composite membranes with micrometer-scale methanol-barrier layer, the Nafion/GO@PDASA-20 membrane possesses an methanol-barrier layer with negligible thickness (20 nm), which has less influence on the proton conductivity. The conductivity of GO@PDASA may be still lower than that of Nafion, but the minimal content of GO@PDASA could not obviously decrease the conductivity of composite membrane.

Table S2, Table S3 and Figure S5 show the selectivities (proton conductivity / methanol permeability) of membranes in literature and in this study. The Nafion/GO@PDASA-20 membrane exhibits a high selectivity of 7.32×10^5 S s cm^{-3}, which is 13.9 times of that of Nafion 212 membrane (5.28×10^4 S s cm^{-3}). This is one of the highest selectivity reported to date for PEMs, which is expected to be beneficial for high-performance DMFC.

The cell performance of the membranes is shown in Fig. 3c. The open circuit voltage (OCV) and maximum power density are 0.616 V and 25.65 mW cm^{-2}, respectively, for the cell using Nafion 212 membrane. The OCV increases to 0.682 (for Nafion/GO-20), 0.695 (for Nafion/GO@PDASA-10), 0.705 (for Nafion/GO@PDASA-20), 0.712 (for Nafion/GO@PDASA-30), and 0.708 V (for Nafion/GO@PDASA-40). With increasing the number of GO@PDASA layers from 0 to 20, the maximum power density rapidly increases to 44.37 mW cm^{-2} (increase by 73%), while the maximum power density increases more slowly with further increasing the GO@PDASA layers to 40 (reaching 49.78 mW cm^{-2}). This variation tendency is significantly in accordance with the increase of selectivities. The enhanced cell performance is due to the decreased methanol permeability and sufficiently high proton conductivities. Moreover, the GO membranes may be advantageous for the close contact between catalyst layer and the composite membrane, leading to further increase of cell performance.

In summary, we propose a novel strategy to fabricate highly proton-conducting, methanol-blocking membrane through spin-coating an ultrathin crosslinked sulfonated GO film (~20 nm) on Nafion support. The resulting Nafion/GO@PDASA-20 membrane overcomes the tradeoff effect: 93% decrease of methanol permeability while retaining the high proton conductivity of Nafion, owing to the synergistic optimization of methanol-transport and proton-transport channels within the GO film. This study offers guidelines for rational design of methanol-blocking film on PEMs to surpass the tradeoff hurdle: (i) the topological structure of transport channels should be tuned to block methanol diffusion *via* size exclusion effect as well as be highly continuous to afford high proton mobility; (ii) the chemical microenvironment of transport channels should be tuned to afford high proton concentration.

We thank the financial support from the National Science Fund for Distinguished Young Scholars (21125627), and the Program of Introducing Talents of Discipline to Universities (B06006).

Notes and references

[a] Key Laboratory for Green Chemical Technology of Ministry of Education, School of Chemical Engineering and Technology, Tianjin University, Tianjin 300072, China.
[b] Collaborative Innovation Center of Chemical Science and Engineering (Tianjin), Tianjin 300072 China

† Electronic Supplementary Information (ESI) available: Experimental section, AFM, XRD, XPS and FTIR of GO, SEM image of Nafion 212, XRD of the membranes, water uptake, proton conductivity, comparisons of conductivity, methanol permeability and selectivity. See DOI: 10.1039/c000000x/

1. G. He, Z. Li, J. Zhao, S. Wang, H. Wu, M. D. Guiver and Z. Jiang, *Adv. Mater.*, 2015, **27**, 5280-5295.
2. K.-D. Kreuer, *Chem. Mater.*, 2014, **26**, 361-380.
3. L. Robeson, H. Hwu and J. McGrath, *J. Membr. Sci.*, 2007, **302**, 70-77.
4. R. R. Nair, H. A. Wu, P. N. Jayaram, I. V. Grigorieva and A. K. Geim, *Science*, 2012, **335**, 442-444.
5. H. W. Kim, H. W. Yoon, S. M. Yoon, B. M. Yoo, B. K. Ahn, Y. H. Cho, H. J. Shin, H. Yang, U. Paik, S. Kwon, J. Y. Choi and H. B. Park, *Science*, 2013, **342**, 91-95.
6. H. Li, Z. Song, X. Zhang, Y. Huang, S. Li, Y. Mao, H. J. Ploehn, Y. Bao and M. Yu, *Science*, 2013, **342**, 95-98.
7. R. K. Joshi, P. Carbone, F. C. Wang, V. G. Kravets, Y. Su, I. V. Grigorieva, H. A. Wu, A. K. Geim and R. R. Nair, *Science*, 2014, **343**, 752-754.
8. L. Sha Wang, A. Nan Lai, C. Xiao Lin, Q. Gen Zhang, A. Mei Zhu and Q. Lin Liu, *J. Membr. Sci.*, 2015, **492**, 58-66.
9. G. He, C. Chang, M. Xu, S. Hu, L. Li, J. Zhao, Z. Li, Z. Li, Y. Yin, M. Gang, H. Wu, X. Yang, M. D. Guiver and Z. Jiang, *Adv. Funct. Mater.*, 2015, DOI: 10.1002/adfm.201503229.
10. I. Nicotera, C. Simari, L. Coppola, P. Zygouri, D. Gournis, S. Brutti, F. D. Minuto, A. S. Aricò, D. Sebastian and V. Baglio, *J. Phys. Chem. C*, 2014, **118**, 24357-24368.
11. C. W. Lin and Y. S. Lu, *J. Power Sources*, 2013, **237**, 187-194.

12. H. W. Kim, H. W. Yoon, B. M. Yoo, J. S. Park, K. L. Gleason, B. D. Freeman and H. B. Park, *Chem. Commun.*, 2015, **50**, 13563-13566.
13. J. Zhao, Y. Zhu, F. Pan, G. He, C. Fang, K. Cao, R. Xing and Z. Jiang, *J. Membr. Sci.*, 2015, **487**, 162-172.
14. S. P. Jiang, Z. Liu and Z. Q. Tian, *Adv. Mater.*, 2006, **18**, 1068-1072.
15. G. He, L. Nie, X. Han, H. Dong, Y. Li, H. Wu, X. He, J. Hu and Z. Jiang, *J. Power Sources*, 2014, **259**, 203-212.

